Chapter 31

Electron Transfer in Photosynthetic Reaction Centers

Josef Wachtveitl*
Institut für Physikalische und Theoretische Chemie, Goethe-Universität Frankfurt, 60439 Frankfurt, Germany

Wolfgang Zinth
Sektion Physik, Ludwig-Maximilians-Universität München, Oettingenstr. 67, 80538 München, Germany

Summary

The central importance of (bacterio)chlorophyll as a major photosynthetic pigment arises from its ability to both harvest the sunlight and perform ultrafast electron transfer (ET) reactions. The main function of the reaction center (RC) is to convert the photoexcitation in order to generate a trans-membrane potential in a series of ET steps. In bacterial RCs it is possible to relate molecular structure and biological function by exploring the early events after photoexcitation. In a series of ultrafast time resolved experiments with native and modified samples, the details of the primary photosy nthetic reactions become visible, information on the relevant electron transfer parameters (free energy, reorganization energy and electronic coupling) can be deduced. This leads to a better understanding of architectural principles in photosynthetic RCs and optimization strategies in photosynthesis.

*Author for correspondence, email: wveitl@theochem.uni-frankfurt.de

Bernhard Grimm, Robert J. Porra, Wolfhart Rüdiger and Hugo Scheer (eds): Chlorophylls and Bacteriochlorophylls: Biochemistry, Biophysics, Functions and Applications, pp. 445–459.

I. Introduction

The early events in photosynthesis are the absorption of a photon by the light harvesting antenna systems, followed by a rapid and efficient transfer of the excitation energy to the reaction center (reviewed in the preceding two chapters of this book), where the primary charge separation takes place. The general energy storage principle of the photosynthetic reaction center (RC) is to link electron transfer to directional proton transfer and thus generate a trans-membrane potential. The separation of electrons is established in (bacterio)chlorophyll ((B)Chl) containing pigment-protein complexes embedded in the photosynthetic membrane. A series of fast electron transfer (ET) reactions, along a chain of pigment molecules and across the photosynthetic membrane, stabilizes the electrochemical charge separation energy.

In oxygenic photosynthetic organisms, two photosystems (PS I and PS II) act in concert to transfer electrons from water to $NADP^+$. After the purple bacterial RC (Deisenhofer et al., 1984; Allen et al., 1987; Chang et al., 1991; Ermler et al., 1994; Stowell et al., 1997), PS I is the second type of photosynthetic RC for which the X-ray structure was solved with high resolution (Jordan et al., 2001; Ben-Shem et al., 2003). The structural data provide a detailed picture of the cofactor arrangement and, therefore, the basis for an assignment of the sequence of ET steps spectroscopically detected in PS I (Fig. 1, left) (Brettel and Leibl, 2001). The main experimental difficulty for time resolved optical spectroscopy is the fact, that PS I preparations are usually associated with their antenna systems, i.e., they contain approx. 100 chlorophyll molecules. Thus, the absorbance changes following photoexcitation contain both energy and electron transfer components, because both processes occur on the same time scale. Since the contribution of the antenna chlorophylls is approx. one order of magnitude larger (Savikhin et al., 2000), it is impossible to directly detect the first charge separated intermediate, $P700^+A_0^-$, in intact PS I preparations and the determination of the intrinsic time constants of primary reactions has to rely on indirect methods (Beddard, 1998; Brettel, 1997). Although for these reasons, the time constant for the formation of the first ET intermediate $P700^+A_0^-$ is not well established, values of a few picoseconds are reported in the literature (Byrdin et al., 2000; Savikhin et al., 2000). These ET rates can now be compared with the cofactor distances derived from the X-ray structure. An edge-to-edge distance of 13 Å between P700 and A_0 would lead to an estimated ET rate in the order of 10^7, i.e., 5 orders of magnitude slower than the one observed. This discrepancy can be overcome by assuming an active role for the chlorophylls eC-B2 (and/or eC-A2), located between P700 and A_0, as real electron transfer intermediate (reviewed in Brettel and Leibl, 2001). This discussion is reminiscent of the long standing debate concerning the role of the 'accessory' chlorophylls in bacterial RCs, which will be addressed in detail below.

Also, for PS II, electron and energy transfer processes are hard to disentangle. Although PS II reaction centers containing only six Chl molecules per complex can be isolated, the similar Chl couplings, and hence the lack of an isolated, low-lying excited state, complicate the assignment of the femto- and picosecond transients (Prokhorenko and Holzwarth, 2000). This supermolecular behavior can be described satisfactorily by a Multimer Model (Barter et al., 2003) that reproduces the experimental data in agreement with the medium resolution PS II structure (Jordan et al., 2001; Vasil'ev et al., 2001; Bibby et al., 2003).

In this chapter the discussion of primary electron transfer will be focused on purple bacterial RC. These systems can be prepared devoid of any antenna chlorophylls and show a largely unidirectional electron transfer. Thus, the integrated approach of structural analysis, ultrafast spectroscopy and protein (and/or pigment) modification allows a direct and detailed analysis of the early photosynthetic light reactions.

II. Dynamics and Energetics of the First Electron Transfer Reactions in Bacterial Reaction Centers

The experimental prerequisite for the time resolved observation of the fast ET dynamics within the RC is the synchronization of the reaction by an even faster external trigger. Femtosecond spectroscopy

Abbreviations: $B_{A/B}$ – sites of monomeric BChl in the RC (A and B refer to the position on the active and inactive branch, respectively); *Blc.* – *Blastochloris*; Cyt – cytochrome; ET – electron transfer; $H_{A/B}$ – sites of monomeric BPhe in the RC; P – primary electron donor; P_+P_- – upper/lower exciton band of P; P^+ – cation radical of P (note: in all ion radicals the dot is omitted, i.e., B^-, H^- instead of $B^{\bullet-}$, $H^{\bullet-}$; $Q_{A/B}$ – quinone sites; *Rba.* – *Rhodobacter*; RC(s) – reaction center(s); V – electronic coupling; ΔG – gain in free energy; λ – reorganization energy; λ_{pr} – probing wavelength

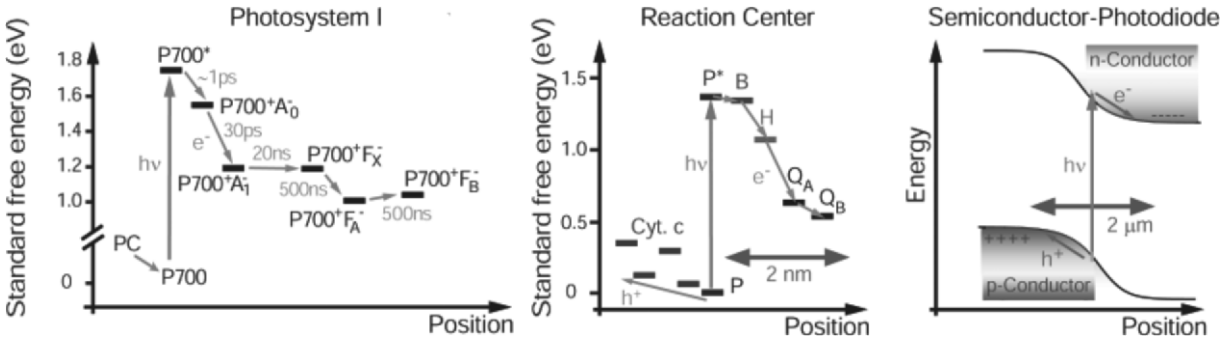

Fig. 1. Energetics of ET systems. left: PS I, middle: bacterial RC, right: semiconductor photodiode. For PS I the ET kinetics, electron pathways and energetics of ET intermediates are still under debate, the schematic arrangement and the energetic positions of the cofactors, as recently discussed in Brettel and Leibl (2001), is depicted on the left. The primary electron donor P700 is a dimer of Chl *a* and the chain of electron acceptors consists of a Chl *a* monomer (A_0), a phylloquinone (A_1) and three [4Fe-4S] clusters (F_X, F_A and F_B). The ET steps for purple bacterial RC from *Blc. viridis* (center) are discussed in detail in the text. The photoprocesses taking place in the reaction centers resemble those in a photodiode (right). In all systems light absorption is followed by fast charge separation processes involving both electron and hole transfer. See also Color Plate 6, Fig. 2.

with pulses in the range of a few 10 fs allows a direct observation (i) of the sequence of ET steps following the photoexcitation of the primary donor P in native and modified RC (Sections A and B) and (ii) of even initial nuclear motions via vibrational wave packet evolution (Section C).

A. The Primary Electron Acceptor, Energetics of the First Intermediate State $P^+B_A^-$

Since the successful resolution of the molecular structure of bacterial reaction centers (Deisenhofer et al., 1984; Allen et al., 1987), the individual chromophores within the protein can be directly related with the various primary photochemical events (Fig. 2). The RCs in purple bacteria consist of at least three protein subunits (L, M and H), four BChl and two BPhe molecules, one atom of non-heme ferrous iron and two quinone molecules. Most investigations on purple bacterial photosynthesis were carried out on *Rhodobacter* (*Rba.*) *sphaeroides, Rba. capsulatus* (which contain BChl *a* as tetrapyrroles) and *Blastochloris* (*Blc.*) *viridis* (which contain BChl *b*). The chromophores are arranged in two branches (termed A and B) with an approximate C_2-symmetry. Two BChl molecules are strongly coupled electronically and represent the primary electron donor P. Over the last two decades, the dynamics of the electron transfer steps following the light-induced generation of the excited electronic state P* has been studied by time-resolved spectroscopy. The most prominent kinetic component is the decay of the P*-state and the

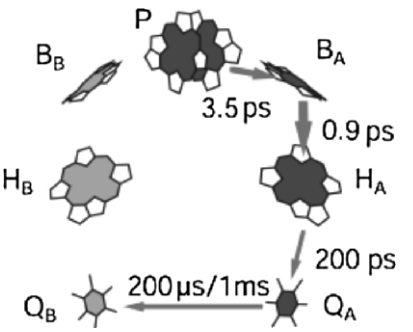

Fig. 2. Scheme of chromophore arrangement and reaction dynamics of primary electron transfer steps in the bacterial RC. ET proceeds via the active branch of electron carriers consisting of the special pair P, the BChl B_A, the BPhe H_A and the quinones Q_A and Q_B. The electron is transferred from P to Q_A within 200 ps, the $Q_A \rightarrow Q_B$ transition is approx. 10^6-fold slower. Recent FTIR-studies report that Q_B is not directly reduced by Q_A^-, but through an intermediary electron donor (Remy and Gerwert, 2003). According to these data, the main time constants are 150 µs for Q_B reduction and 1.1 ms for Q_A reoxidation.

formation of the product state $P^+H_A^-$ within ~ 3 ps at room temperature (Woodbury et al., 1985; Breton et al., 1986; Martin et al., 1986; Holzapfel et al., 1989, 1990; Dressler et al., 1991). Polarized spectroscopy on crystallized RCs (Zinth et al., 1983; Knapp et al., 1985) and time-resolved analysis based on spectral differences of H_A and H_B at low temperatures (Kirmaier et al., 1985; Michel-Beyerle et al., 1988) demonstrated that predominantly the A-branch is active in electron transfer. Advanced spectroscopic methods revealed details of the P* state, like the species-dependent degree of intradimer charge transfer character (of the type $P_L^+P_M^-$) (Lathrop and Friesner,

1994; Rautter et al., 1994) or the apparent deviations from a mono-exponential decay (Du et al., 1992; Hamm et al., 1993; Jia et al., 1993; Ogrodnik et al., 1994; Beekman et al., 1995).

Individual ET steps in the photosynthetic systems are often explained in the frame of Marcus theory (Marcus and Sutin, 1985; Moser et al., 1993). In the simplified description, four parameters control each reaction step: the electronic coupling V between the donor and acceptor molecules, the gain in free energy ΔG, the reorganization energy λ and the vibrational frequency ω, which is taken as a measure for the temporal modulation of the energy gap between donor and acceptor states induced by the molecular motion.

Inspection of crystallographic data and the effect of magnetic fields allowed exclusion of the direct reaction $P^* \rightarrow P^+H_A^-$, since the rate predicted by classical nonadiabatic Marcus theory would be several orders of magnitude too slow. Therefore, an active role of the monomeric chlorophyll B_A, either as virtual intermediate via a superexchange mechanism (Bixon et al., 1989, 1991), or as a real, transiently populated intermediate, appeared likely. A sequential electron transfer via B_A imposes not only restrictions on the energetics of the intermediate $P^+B_A^-$ (as will be discussed below), but also on its dynamics. The similar kinetics observed for P* decay and $P^+H_A^-$ formation requires that the decay of the intermediate, $P^+B_A^-$, must be significantly faster than its formation. Under that condition, only a small transient population of the $P^+B_A^-$ intermediate results (Marcus, 1987). This fact rendered the direct observation of the $P^+B_A^-$ state difficult; but, in a series of experiments, a distinct subpicosecond kinetic component could be identified (Holzapfel et al., 1989, 1990; Chan et al., 1991; Dressler et al., 1991; Arlt et al., 1993; Beekman et al., 1995). The amplitude of this component is especially pronounced in spectral regions with high BChl and $BChl^-$ absorption. The most suitable region for the unambiguous detection of the subpicosecond component is the near-IR absorption band of the monomeric BChl radical anion (in *Rba. sphaeroides* at 1020 nm (Fajer et al., 1975; Fujita et al., 1978)). Here, contributions from ground state absorption and stimulated emission are so small, that the transient absorption changes at early delay times can be modeled exclusively with a 0.9 ps time constant (Fig. 3, open circles). Photodichroism provides another critical test of the sequential reaction model. The transient absorption data in Fig. 3 reveal a change in

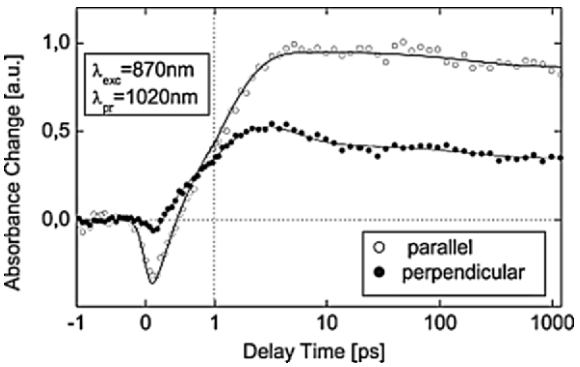

Fig. 3. Polarization dependent transient absorption kinetics in the BChl *a* radical anion band of native *Rba. sphaeroides* RCs. Open/filled circles: parallel/perpendicular polarization of pump and probe pulses. The model curves (lines) are calculated using time constants of 0.9 ps, 200 ps and infinity for parallel polarization and an additional 3 ps component for perpendicular polarization (modified after Wachtveitl et al., 1998). The time scale is linear for delay times $\tau_d < 1$ ps and logarithmic for $\tau_d < 1$ ps.

the dichroic ratio $A_\parallel/A_\perp$ with delay time. This readily indicates that different intermediates with dissimilar direction of their transition dipole moments are involved in the electron transfer chain. The sequential model including a real $P^+B_A^-$ intermediate leads to an agreement within a few degrees between the spectroscopic data and the angle between the Q_Y transitions of P and B_A^- as predicted by the X-ray structure (Arlt et al., 1993; Wachtveitl et al., 1998).

B. Specific Variation of Electron Transfer Parameters by Protein Engineering and Chromophore Modification

Since more than a decade, selective perturbations of the RC pigment-protein complex can be introduced by site-directed mutagenesis (Bylina and Youvan, 1988; Coleman and Youvan, 1990; Gray et al., 1990; Farchaus et al., 1993) or by pigment exchange (Struck and Scheer, 1990; Struck et al., 1990; Meyer and Scheer, 1995). The modifications allow us to address specific regions of the ET chain and result in a variation of the relevant parameters controlling ET dynamics.

1. The Primary Donor P

A series of mutants was designed to modify the environment of the primary electron donor P (Wachtveitl et al., 1993; Allen et al., 1996; Kuglstatter et al., 1999; Schenkl et al., 2002). It could be shown that a change

Table 1. Electron transfer properties for native and mutated *Blc. viridis* reaction centers at room and low temperatures

RC *Blc. viridis*	$\Delta U_{P/P}$+ [mV]	$\Delta\Delta G$ [cm^{-1}]	room temperature			low temperature 1) 30 K; 2) 50 K	
			τ_1 [ps]	τ_{1A} / τ_{1B} [ps]	$R = \frac{a(\tau_{1A})}{a(\tau_{1B})}$	τ_{1A} / τ_{1B} [ps]	$R = \frac{a(\tau_{1A})}{a(\tau_{1B})}$
WT	0	0	3.5 ± 0.4	1.8 / 7.4	1.4	1.1 / 37[1)]	2.9
L168HF	–80	–670	1.1 ± 0.2	0.8 / 3.8	4.8	0.25 / 1.7[1)]	1.9
M195YF	–45	–370	3.1 ± 0.3	1.5 / 5.4	0.8	1 / 3.5[2)]	3.3
L168HF/M195YF	–80	*	0.8 ± 0.2	0.6 / 3.2	3.0	–	–
M195YH	+20	+170	5.7 ± 0.5	3.5 /14.5	2.0	–	–
L181FY	–25	–210	1.7 ± 0.2	1.15/ 4.5	2.8	0.5 / 1.3[2)]	2.5
M208YF	+15	*	20 ± 3	8 /30	0.3	9 / 83[1)]	0.44
M208YL	+15	*	29 ± 5	11 / 50	0.5	–	–
L181FY/M208YF	–25	*	8.2 ± 1.5	4.5 / 16	2.3	–	–
L153HC	+2	+16	3.8 ± 0.4	2.5 / 10	3.0	–	–
L153HE	–	*	12 ± 1	7 / 40	2.0	–	–
L153HL	0	–1600	3.5 ± 0.4	3 / 43	4.0	–	–
L162YF	≈–5	–40	3.5 ± 0.4	2.7/ 16	>4.0	–	–
L162YG	+10	+80	5.4 ± 0.5	3.3/ 18	2.6	–	–

The P/P^+- redox midpoint potential ($\Delta U_{P/P}$+) is expressed as difference from the WT value of +520 mV (vs.NHE). This value together with the contribution arising from chromophore modification (e.g., BPhe *b* instead of BChl *b* at B_A position in L153HL RC) determines the change in free energy difference for the first electron transfer step. * $\Delta\Delta G$ cannot be calculated explicitly for these cases since additional changes are expected. The given decay constants result from a monoexponential (τ_1) or a biexponential (τ_{1A}, τ_{1B}) fit of the first electron transfer step $P^* \rightarrow P^+B_A^-$. R indicates the ratio of the respective amplitudes.

of the hydrogen bonding pattern between the two BChls constituting P and the protein is closely correlated to the oxidation potential of the primary donor (Lin et al., 1994; Wachtveitl et al., 1998). However, the altered driving force between donor and acceptor does not influence the ET rates in the way expected from the direct application of Marcus theory (Williams et al., 1992; Schenkl et al., 2002). This deviation was confirmed in fs-experiments on various mutant RCs at different temperatures (Huppmann et al., 2002). It is found, that different site specific mutant RCs can vary in their rate of the primary charge separation by more than one order of magnitude (Zinth et al., 1998; Huppmann et al., 2002). These results readily indicate that the kinetic picture is more complicated than a simple chromophore distance vs. log (k_{ET}) relationship (Moser et al., 1992). In Table 1 spectroscopic, redox and dynamic properties of native and mutated RC of *Blc. viridis* are compared. Under the often used assumption that the mutation predominantly influences the energetics of the primary electron transfer intermediates, the primary charge separation steps at room temperature can be modeled according to nonadiabatic ET-theory, if the single mode model is expanded and an additional high frequency mode (ω_h = 1500 cm^{-1}) is considered. This 'multi'mode treatment is necessary to explain the fast charge separation for mutant RCs, where the mutation pushes the primary reaction far into the Marcus inverted region (e.g., for L153HL). This procedure yields a value of 600 ± 200 cm^{-1} for the reorganization energy λ, an electronic coupling V = 37 ± 10 cm^{-1} and a free energy gap ΔG ranging from –600 to +800 cm^{-1} (Zinth et al., 1998; Huppmann et al., 2002, 2003). Interestingly, the primary reaction for native RCs appears to be slightly activated within this model (Huppmann et al., 2002). Consequently, several mutant RCs with a significantly accelerated primary reaction could be constructed (Table 1), especially by removing a hydrogen bond to the special pair P (L168HF, M195YF and L168HF/M195YF). Interestingly, such a strong acceleration was not observed for the corresponding mutants in *Rba. sphaeroides* (Murchison et al., 1993; Woodbury et al., 1994).

The classical Marcus treatment (Marcus and Sutin, 1985) results in a significant activation energy for

the primary ET reaction of native and some mutant RCs in *Blc. viridis* (e.g., $E_A \approx 180$ cm^{-1} for wild type RCs). Consequently, an Arrhenius-type temperature dependence, where the reaction slows down at reduced temperatures, is expected for these RCs. However in most RCs (except M208 mutants) an accelerated charge separation towards low temperatures (requiring negligible activation energies $E_A << \hbar\omega$) is found (Breton et al., 1988; Fleming et al., 1988; Lauterwasser et al., 1991; Huppmann et al., 2002). An improved description of ET in proteins therefore needs to consider not only different values for the energetics but also specific variations of other ET parameters upon mutation and temperature change. Especially the electronic coupling V is highly sensitive to subtle conformational changes and drastically affects the primary ET dynamics (McMahon et al., 1998; Zhang and Friesner, 1998; Kolbasov and Scherz, 2000). A modulation of the electronic coupling V with mutation is able to explain a number of observations. However, the strong acceleration of reaction rates upon cooling, found in many RC requires a different explanation. An increase of V upon cooling can consistently explain the fs data. Such a temperature dependence might even reflect more general dynamic properties of proteins: at high temperatures, protein motions have large amplitudes and cause local disorder, which results in a high entropic term and in large fluctuations of the donor/acceptor geometry away from the optimum required for fast ET. This may lead to relatively weak average electronic coupling. At low temperatures the protein is locked in a state with low entropy and high electronic coupling V leading to faster ET dynamics for the case of photosynthetic RCs.

In general, a quantitative description of the effect of a mutation or of the temperature dependence of the various ET-processes in photosynthetic reaction centers spanning a broad range cannot be obtained without a variation of the relevant ET parameters. A decrease in electronic coupling V with temperature is highly probable.

2. The Primary Acceptors B_A and H_A

Except for the BChl *a* dimer P, all tetrapyrroles in the *Rba. sphaeroides* RC are accessible to pigment exchange (Meyer and Scheer, 1995). With exchange rates as high as 90% or better, pigment-modified RCs are, therefore, especially suited to tune the

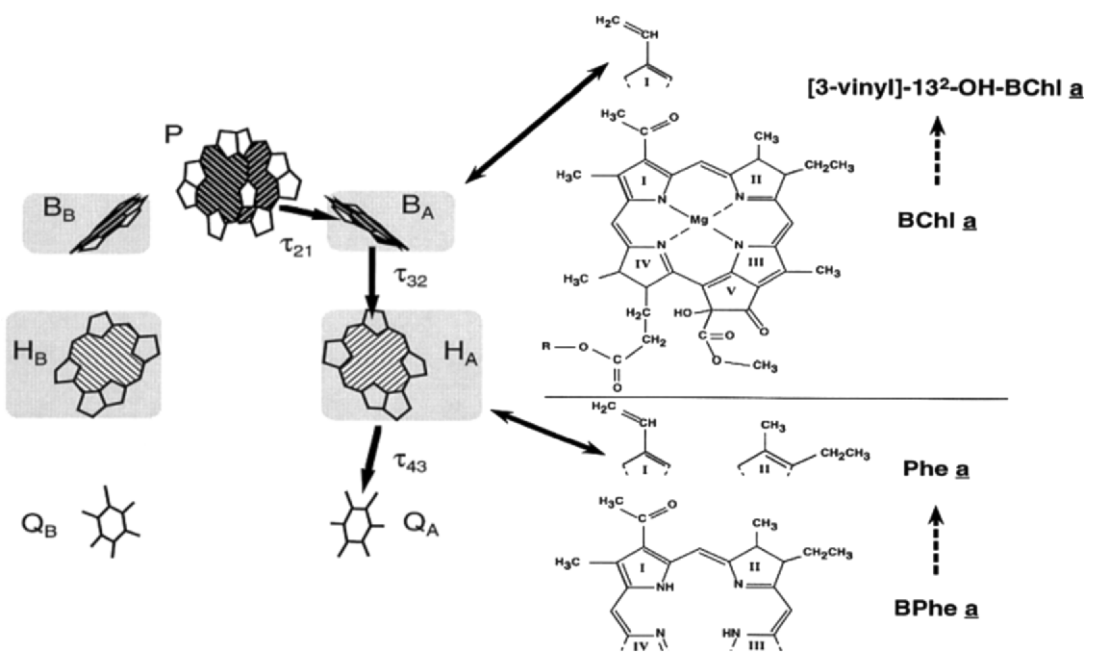

Fig. 4. Sites of pigment exchange (gray boxes) in the RC of *Rba. sphaeroides* (left) and structural differences between the native and the site-specifcally introduced modified pigments (right); modified after Spörlein et al. (2000). Rings I, II, III, IV and V are known as Rings A, B, C, D and E, respectively, in the IUB-IUPAC nomenclature system used elsewhere in this book. The 13^2-OH group in [3-vinyl]-13^2-OH-BChl *a* does ot interfere with electron transfer.

energy levels of the electron acceptors B_A and H_A without changes in the protein moiety (Fig. 4). The introduction of plant pheophytin (Phe *a*) into the H_A and H_B sites, replacing the BPhe *a* molecules, drastically alters the primary reaction dynamics (Shkuropatov and Shuvalov, 1993; Schmidt et al., 1994, 1995) and allowed the final proof of stepwise ET with the accessory BChl as a real electron carrier: a reduced quantum yield (Franken et al., 1997) and a long lived population of the $P^+B_A^-$ intermediate was observed (Fig.5). Since the redox potential of Phe *a* is considerably more negative (≈ 220 mV) than that of BPhe *a* (Geskes et al., 1995) the exchange results in an energetic proximity between the $P^+B_A^-$ and $P^+H_A^-$ intermediates. Forward and backward rates, according to the scheme depicted in Fig. 5 (top), are determined by the free energy difference ΔG of the different intermediate states and can be correlated by the principle of detailed balance (Schmidt et al., 1994, 1995). This procedure allowed the determination of the free energy difference between P* and $P^+B_A^-$ (ΔG ≈ 450 cm^{-1}). A similar value for the free energy difference was determined in recombination fluorescence measurements, where ΔG (P^*-$P^+B_A^-$) = 550 cm^{-1}

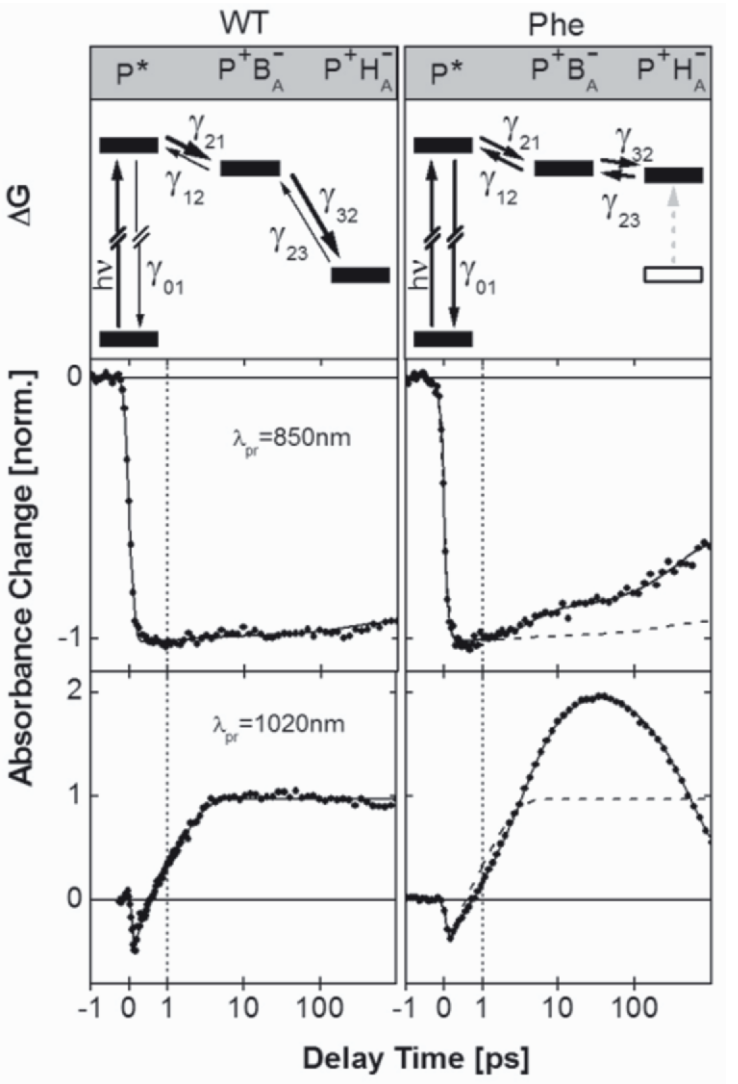

Fig. 5. Schematic representation of the energetic positions of the electron transfer intermediates and the corresponding microscopic time constants (top) for native (left) and Phe *a* containing RC. Transient absorbance changes for spectral regions with dominant contributions from ground state bleaching (middle) and BChl anion absorption (bottom).

(Shuvalov and Yakovlev, 2003). The temperature dependence of the charge separation in Phe *a* containing RC confirmed a ΔG (P^*-$P^+B_A^-$) value in this range; but, as discussed above, it also showed the necessity for an expansion of the simple Marcus picture by temperature-dependent parameters to consistently explain the low temperature data (Huber et al., 1998). As indicated in Fig. 4, BPhe *a* and Phe *a* differ in their chemical structures in two positions, that is the saturation of ring II (B) and the peripheral group at the C-3 position. The role of each variation can be addressed individually with RCs containing [3-vinyl]-BPhe *a* and [3-acetyl]-Phe *a* at the H_A and H_B positions. It was found that spectral and dynamic properties can be separated from each other in the sense, that the ring II (B) conjugation is responsible for the spectral shift between BPhe *a* and Phe *a*, whereas the C-3 substituent controls the efficiency of the primary reaction via optimization of the redox potential (Huber et al., 1995).

A systematic variation of the free energy could also be achieved for the primary electron acceptor B_A. The effect of an energetically elevated acceptor level, as expected for [3-vinyl]-BChl *a* RCs is, again, in accord with a stepwise electron transfer model: here, a slower and less efficient charge separation accompanied by a significant reduction of $P^+B_A^-$ population is found (Spörlein et al., 2000). This again underlines the fact that the ET chain in the bacterial RC represents a highly optimized system where alterations in pigment composition with the related changes of the energetics of the ET intermediates enhance the various loss mechanisms and, thus, reduce efficiency (Section IV).

C. Alternative Pathways and Vibrational Coherence

In a photosynthetic system, the RC is usually excited by energy transfer from the antenna system(s). The situation that P* is not directly produced by the incident light, but by energy transfer from other pigments, can be mimicked in isolated RCs by photoexcitation of the energetically higher lying states B*, H* or P^*_+ (upper exciton band of P). As expected, fast energy transfer to the lowest excited state P^* occurs within 50–200 fs and the electron transfer proceeds from there as described above (van Grondelle et al., 1994; Stanley et al., 1996; Vos et al., 1997). However, alternative electron transfer pathways also following B* and H* excitation (with laser pulses at 800 nm and 760 nm, respectively) — e.g., an intermediate with $B_A^+H_A^-$ character — were reported for mutant (van Brederode et al., 1997a,b) and wild type RCs (van Brederode et al., 1997b; Vos et al., 1997; S. Lin et al., 1998). Nevertheless, the lack of a $B_A^+H_A^-$ intermediate in a P-deficient mutant (Jackson et al., 1997) demonstrates the requirement for P for stable charge separation. The observation of the alternative reaction path may be of major importance for the understanding of photosynthesis in higher organisms, where the degeneracy of the Q_y transitions of the different pigments and the arrangement of the energy transducing Chl, prevent the predominant excitation of the special pair. Furthermore, the 'accessory' Chl in the active branch of the PS II core is suggested to act as the primary electron donor (Prokhorenko and Holzwarth, 2000; Barter et al., 2003).

Excitation of P with a fs laser pulse shorter than a vibrational period leads to a coherent excitation of vibrational nuclear motions. Quantum mechanically, this is described as a superposition of wavefunctions of several vibrational levels. Figure 6 illustrates the preparation and subsequent evolution of such a wave packet. Therefore, it is a quite common feature in ultrafast experiments that femtosecond kinetics are superimposed with oscillatory components (Rosker et al., 1986; Mokhtari et al., 1990; Wang et al., 1994). Thus, the first observations of vibrational coherence in photosynthetic reaction centers (Vos et al., 1991, 1993, 1994; Streltsov et al., 1997) immediately raised the question about a possible functional role of these coherent nuclear motions for photosynthetic electron transfer (reviewed in Vos and Martin, 1999). The first oscillatory components, with the strongest modes occurring in the $<100\ cm^{-1}$ region, were modulations of the stimulated emission from P* (Vos et al., 1991, 1993). Experiments probing the stimulated (Vos et al., 1994) and the spontaneous emission of P* (Stanley and Boxer, 1995) both gave similar results, and led to the assignment that the activated modes originate from the motion of a vibrational wave packet on the P* potential energy surface. The vibrational modes around $100\ cm^{-1}$ are usually considered as chromophore vibrations or as chromophore driven protein motions. Molecular dynamics simulations (Warshel, 1980), and observations of similar low-frequency modes in other non-monomeric BChl assemblies (like antenna complexes) (Chachisvilis and Sundström, 1996; Joo et al., 1996; Monshouwer et al., 1997; Diffey et al., 1998), suggest a strong contribution from intradimer vibrational modes (Kumble et al., 1996).

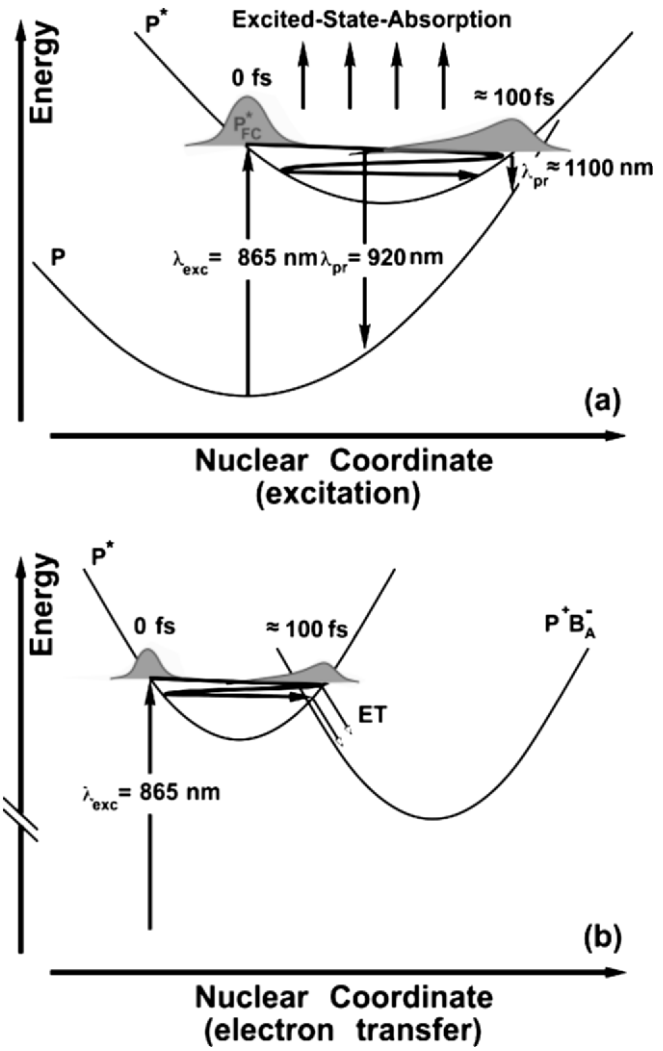

Fig. 6. Scheme to visualize oscillatory absorption changes via the modulation of stimulated emission (a) and modulated ET (b). (a) Wavepacket evolution on a one-dimensional representation of the excited state potential energy surface. The values given describe the energetic and dynamic properties in RCs from *Rba. sphaeroides*. After excitation (865 nm) from the ground state (P) in the Franck-Condon region of the excited state (P^*_{FC}), the created wavepacket moves on the potential energy surface P*. Since excited-state-absorption occurs as long as this state is populated, it is detectable instantaneously. After a few tens of femtoseconds the RC has reached the correct nuclear configuration to allow observation of stimulated emission. Oscillatory modulations of the transients due to the moving wavepacket are observed with different phases at both sides of the spectrum. At 1100 nm the signal of stimulated emission is measurable only for a short time of 250 fs, since at later times relaxation of the wavepacket by energy redistribution prevents the system from reaching this extreme nuclear configuration for a second time. (b) Simplified model for discontinuous electron transfer: after excitation, the wavepacket oscillates on the potential energy surface of P*. It is assumed that a considerable probability of transfer exists only in a small range of nuclear configurations. Each time the wavepacket reaches the intersection region of electron donor (P*) and acceptor ($P^+B_A^-$) there is a possibility to access the $P^+B_A^-$ surface. Therefore the P* state will be depopulated stepwise due to the wavepacket motion. The oscillations of the P* population should not change phase.

The question, if the dominant mode around 100 cm^{-1} is coupled to electron transfer, can be addressed experimentally in the spectral region covering both the electron donor and acceptor bands (Spörlein et al., 1998). Model calculations for the case of a stepwise depopulation of P* and a subsequent population of $P^+B_A^-$ (Fig. 6b), suggest a much stronger modulation of the $P^+B_A^-$ signal compared to the P* signal. In contrast to these expectations for a wave-packet-like modulation of the ET process, the features of the os-

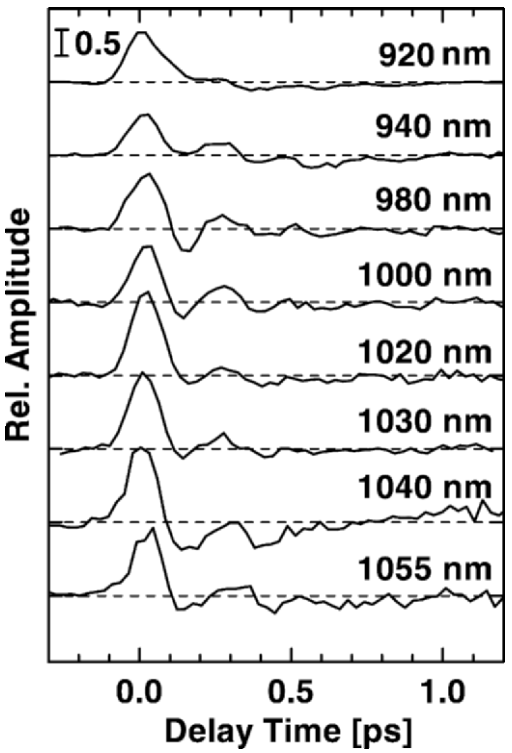

Fig. 7. Residuals from *Rba. sphaeroides* RCs obtained by subtracting a fit curve satisfying the exponential characteristics of the transients from experimental data. They reflect the nuclear motions in real time. The spectral range displayed covers both the stimulated emission band of P* and the absorption band of B_A^-. To allow a better comparison, the plotted graphs are normalized to the amplitude of stimulated emission, which decreases with probing wavelength (taken from Spörlein et al., 1998).

cillatory residuals (Fig. 7) do not change significantly within the B_A^--band (centered at 1020 nm). They can be readily explained by the motion of a vibrational wave packet on the excited state potential surface of the special pair P* and its effect on stimulated emission and excited state absorption, without employing a stepwise electron transfer (Spörlein et al., 1998). The spectral analysis of the residual signals revealed a dominant mode with 135 cm^{-1}, which is damped on the sub-ps time scale, and a weak 40 cm^{-1} mode for λ_{pr} <1030 nm. The involvement of such a low frequency (~30 cm^{-1}) mode in the coherent formation of $P^+B_A^-$ was previously suggested (as recently reviewed in Shuvalov and Yakovlev, 2003) and tentatively assigned to a rotation of water molecules bridging ET active chromophores by hydrogen bonds.

Also for *Blc. viridis* RC strong modulations of the kinetics in the region of a dominant stimulated emission signal with a Fourier spectrum similar to the one observed for *Rba. sphaeroides* could be obtained (Huppmann et al., 2003). Again these features cannot be taken as a direct proof for a coupling of coherent nuclear motion to primary electron transfer for the native RC at room temperature.

In conclusion, for the standard situation of non-adiabatic electron transfer reaction only a small transfer probability exists during a single vibrational period. In this case, the frequency ω influences the ET rate only at low temperatures. Theoretical simulations (Parson and Warshel, 1993; Xu and Schulten, 1994) and measurements of the temperature dependence place ω in the range of 70–200 cm^{-1} (oscillation periods in the 170–500 fs range). For these numbers it is apparent, that the first electron transfer step of room temperature RC occurs in the non-adiabatic regime. However, at cryogenic temperatures the nuclear motions become important for the secondary electron transfer from B_A^- to H_A and for the initial electron transfer reaction in mutated RC with an accelerated charge separation (Huppmann et al., 2003). Here adiabatic processes with medium control are involved in the electron transfer reaction.

III. Optimization of Photosynthesis

The photosynthetic RC is highly efficient in charge separation and electron transfer; for example, values as high as 97% have been reported for the quantum yield of $P^+Q_A^-$ formation (Trissl et al., 1990). The extremely high efficiency is closely related to the design of RC, which has to meet different requirements:

(i) Many photosynthetic bacteria inhabit ecological niches shaded by higher photosynthetic organisms. Therefore, they often must utilize light with wavelengths longer than 700 nm, motivating the usage of BChl instead of Chl. While most photosynthetic bacteria capture light between 750 and 870 nm, the antenna system of the bacterium *Blc.viridis* collects photons even at wavelengths beyond 1000 nm with its BChl *b*-containing antenna system.

(ii) The RC must efficiently collect the excitation coming from the antenna. In order to utilize the excitonic energy from the antenna the absorption of the primary donor—the special pair P of the bacterial RC — must be tuned to long wavelengths. This is achieved by proper selection of the type of bacterial chlorophyll (e.g., using BChl *b* in *Blc.*

viridis), the excitonic coupling of the two BChl molecules of the special pair, the arrangement of the chromophores and the interaction with the surrounding amino acids.

(iii) The excitonic excitation collected by the RC must be stored irreversibly in order to minimize back transfer to the antenna and loss by internal conversion in the antenna system. This demand is fulfilled in the bacterial RC, firstly by appropriate tuning of the energetic position of the excited electronic state of the primary donor (its absorption at the red end of the absorption of all chromophores in the RC) and the high excitonic coupling to other pigments. Secondly, the initial charge separation process is fast (≈ 3 ps), followed by an even faster (≈ 0.6 – 0.9 ps) secondary electron transfer step. In these two processes ≈2000 cm^{-1} of energy are dissipated which prevents a fast back reaction to the antenna.

(iv) The charge separation must be securely maintained before long-time energy storage reactions are accomplished by the later proton transfer processes. Here the RC must minimize the direct charge recombination via electron back transfer to the special pair. This is accomplished by the special design of the electron transfer pathway in the RC: the active branch of electron carriers (see Fig. 2) consists of the special pair P, the BChl B_A, the BPhe H_A and the quinones Q_A and Q_B, arranged in a linear chain. After initial charge separation between P and B_A within 3 ps, the electron travels over the pigment chain in stepwise fashion. The reaction speed decreases with distance from the special pair. The energy of the later intermediate states is also decreased. These two features enable the RC to fulfill the basic requirements for high quantum efficiency in a linear reaction chain: here, for each reaction step, the forward reaction rate must be faster than recombination. The individual optimization criteria are: (a) direct recombination is reduced by increasing the distance between the anion (P^+) and the cation (I^-), and by adjusting the forward reaction rate; and, (b) recombination via earlier intermediates is minimized by appropriate energy decrease for the different reaction steps.

These requirements, together with the standard parameters of the ET reaction in biological systems, determine the arrangement of the electron carriers, the number of intermediate states and the loss in free energy during the electron transfer. In this respect, it is interesting to compare the highly optimized wild type RC with mutated RC. The mutations change reactions rates, absorption properties and energetics of the RCs. In most cases, the reaction rates are reduced and the charge separation efficiency is lowered. In the situation of the mutant L168HF of *Blc. viridis*, where the initial charge transfer reaction is sped up, the absorption spectrum of the special pair is changed and energy transfer from the antenna is strongly reduced. Thus this mutation will not allow the organism to compete with wild type bacteria. It is interesting to note that many mutations lead to reduced quantum efficiencies while still maintaining electron transfer to some degree. This shows that evolutionary design criteria included not only highest quantum efficiency, but also robustness to point mutations and environmental changes.

IV. Concluding Remarks

The solar energy fixation, via charge separation in photosynthesis, is a process where the involved pigment protein complexes — the bacterial RC or the two photosystems PS I and PS II — work with highest efficiency. Structural analysis, ultrafast spectroscopy, site-directed mutagenesis and theoretical modeling have supplied information necessary to describe and to understand the function of the bacterial RC. Here, the interplay of the spatial arrangement and energetic tuning, yield highest quantum efficiency. Despite the elucidation of the molecular structures of PS I and the developing structure of PS II (Zouni et al., 2001; Ferreira et al., 2004), information on the two photosystems PS I and PS II is still incomplete. However, the high similarity of the core pigment arrangement implies that similar design principles are used, and should give some clues how an optimal solar energy converter is built.

References

Allen JP, Feher G, Yeates TO, Komiya H and Rees DC (1987) Structure of the reaction center from *Rhodobacter sphaeroides* R 26 — the cofactors. Proc Natl Acad Sci USA 84: 5730–5734

Allen JP, Artz K, Lin X, Williams JC, Ivancich A, Albouy D, Mattioli TA, Fetsch A, Kuhn M and Lubitz W (1996) Effects of hydrogen bonding to a bacteriochlorophyll-bacteriopheophytin dimer in reaction centers from *Rhodobacter sphaeroides*.

Biochemistry 35: 6612–6619
Arlt T, Schmidt S, Kaiser W, Lauterwasser C, Meyer M, Scheer H and Zinth W (1993) The accessory bacteriochlorophyll: A real electron carrier in primary photosynthesis. Proc Natl Acad Sci USA 90: 11757–11761
Barter LMC, Durrant JR and Klug DR (2003) A quantitative structure-function relationship for the Photosystem II reaction center: Supermolecular behavior in natural photosynthesis. Proc Natl Acad Sci USA 100: 946–951
Beddard GS (1998) Excitations and excitons in Photosystem I. Philos Trans Roy Soc Lond A 356: 421–448
Beekman LM, Visschers RW, Monshouwer R, Heer-Dawson M, Mattioli TA, McGlynn P, Hunter CN, Robert B, van Stokkum IH and van Grondelle R (1995) Time-resolved and steady-state spectroscopic analysis of membrane-bound reaction centers from *Rhodobacter sphaeroides*: Comparisons with detergent-solubilized complexes. Biochemistry 34: 14712–14721
Ben-Shem A, Frolow F and Nelson N (2003) The crystal structure of plant Photosystem I. Nature 426: 630–635
Bibby TS, Nield J, Chen M, Larkum AWD and Barber J (2003) Structure of a Photosystem II supercomplex isolated from *Prochloron didemni* retaining its chlorophyll *a/b* light-harvesting system. Proc Natl Acad Sci USA 100: 9050–9054
Bixon M, Jortner J, Michel-Beyerle ME and Ogrodnik A (1989) A superexchange mechanism for the primary charge separation in photosynthetic reaction centers. Biochim Biophys Acta 977: 273–286
Bixon M, Jortner J and Michel-Beyerle ME (1991) On the mechanism of the primary charge separation in bacterial photosynthesis. Biochim Biophys Acta 1056: 301–315
Breton J, Martin JL, Migus A, Antonetti A and Orszag A (1986) Femtosecond spectroscopy of excitation energy transfer and initial charge separation in the reaction center of the photosynthetic bacterium *Rhodopseudomonas viridis*. Proc Natl Acad Sci USA 83: 5121–5125
Breton J, Martin JL, Fleming GR and Lambry JC (1988) Low-temperature femtosecond spectroscopy of the initial step of electron transfer in reaction centers from photosynthetic purple bacteria. Biochemistry 27: 8276–8284
Brettel K (1997) Electron transfer and arrangement of the redox cofactors in Photosystem I. Biochim Biophys Acta 1318: 322–373
Brettel K and Leibl W (2001) Electron transfer in Photosystem I. Biochim Biophys Acta 1507: 100–114
Bylina EJ and Youvan DC (1988) Directed mutations affecting spectroscopic and electron transfer properties of the primary donor in the photosynthetic reaction center. Proc Natl Acad Sci USA 85: 7226–7230
Byrdin M, Rimke I, Schlodder E, Stehlik D and Roelofs TA (2000) Decay kinetics and quantum yields of fluorescence in Photosystem I from *Synechococcus elongatus* with P700 in the reduced and oxidized state: Are the kinetics of excited state decay trap-limited or transfer-limited? Biophys J 79: 992–1007
Chachisvilis M and Sundström V (1996) Femtosecond vibrational dynamics and relaxation in the core light-harvesting complex of photosynthetic purple bacteria. Chem Phys Lett 261: 165–174
Chan CK, DiMagno TJ, Chen LX, Norris JR and Fleming GR (1991) Mechanism of the initial charge separation in bacterial photosynthetic reaction centers. Proc Natl Acad Sci USA 88: 11202–11206
Chang CH, El-Kabbani D, Tiede D, Norris J and Schiffer M (1991) Structure of the membrane-bound protein photosynthetic reaction center from *Rhodobacter sphaeroides*. Biochemistry 30: 5352–5360
Coleman WJ and Youvan DC (1990) Spectroscopic analysis of genetically modified photosynthetic reaction centers. Annu Rev Biophys Biophys Chem 19: 333–367
Deisenhofer J, Epp O, Miki K, Huber R and Michel H (1984) X-ray structure-analysis of a membrane-protein complex — electron-density map at 3Å resolution and a model of the chromophores of the photosynthetic reaction center from *Rhodopseudomonas viridis*. J Mol Biol 180: 385–398
Diffey WM, Homoelle BJ, Edington MD and Beck WF (1998) Excited-state vibrational coherence and anisotropy decay in the bacteriochlorophyll *a* dimer protein B820. J Phys Chem B 102: 2776–2786
Dressler K, Umlauf E, Schmidt S, Hamm P, Zinth W, Buchanan S and Michel H (1991) Detailed studies of the subpicosecond kinetics in the primary electron transfer of reaction centers of *Rhodopseudomonas viridis*. Chem Phys Lett 183: 270–276
Du M, Rosenthal SJ, Xie X, Dimagno TJ, Schmidt M, Hanson DK, Schiffer M, Norris JR and Fleming GR (1992) Femtosecond spontaneous-emission studies of reaction centers from photosynthetic bacteria. Proc Natl Acad Sci USA 89: 8517–8521
Ermler U, Fritzsch G, Buchanan SK and Michel H (1994) Structure of the photosynthetic reaction-center from *Rhodobacter sphaeroides* at 2.65-Ångstrom resolution — cofactors and protein-cofactor interactions. Structure 2: 925–936
Fajer J, Brune DC, Davis MS, Forman A and Spaulding LD (1975) Primary charge separation in bacterial photosynthesis — oxidized chlorophylls and reduced pheophytin. Proc Natl Acad Sci USA 72: 4956–4960
Farchaus JW, Wachtveitl J, Mathis P and Oesterhelt D (1993) Tyrosine-162 of the photosynthetic reaction-center L-subunit plays a critical role in the cytochrome-c_2 mediated rereduction of the photooxidized bacteriochlorophyll dimer in *Rhodobacter sphaeroides*.1. Site-directed mutagenesis and initial characterization. Biochemistry 32: 12875–12886
Ferreira KN, Iverson TM, Maghlaoui K, Barber J and Iwata S (2004) Architecture of the photosynthetic oxygen-evolving center. Science 303: 1831–1838
Fleming GR, Martin JL and Breton J (1988) Rates of primary electron-transfer in photosynthetic reaction centers and their mechanistic implications. Nature 333: 190–192
Franken EM, Shkuropatov AY, Francke C, Neerken S, Gast P, Shuvalov VA, Hoff AJ and Aartsma TJ (1997) Reaction centers of *Rhodobacter sphaeroides* R-26 with selective replacement of bacteriopheophytin a by pheophytin *a*. 2. Temperature dependence of the quantum yield of $P^+Q_A^-$ and P_3 formation. Biochim Biophys Acta 1321: 1–9
Fujita I, Davis MS and Fajer J (1978) Anion radicals of pheophytin and chlorophyll *a* — their role in primary charge separations of plant photosynthesis. J Am Chem Soc 100: 6280–6282
Geskes C, Meyer M, Fischer M, Scheer H and Heinze J (1995) Electrochemical investigation of modified photosynthetic pigments. J Phys Chem 99: 17669–17672
Gray KA, Farchaus JW, Wachtveitl J, Breton J and Oesterhelt D (1990) Initial characterization of site-directed mutants of tyrosine M210 in the reaction centre of *Rhodobacter sphaeroides*. EMBO J 9: 2061–2070
Hamm P, Gray KA, Oesterhelt D, Feick R, Scheer H and Zinth W

(1993) Subpicosecond emission studies of bacterial reaction centers. Biochim Biophys Acta 1142: 99–105

Holzapfel W, Finkele U, Kaiser W, Oesterhelt D, Scheer H, Stilz HU and Zinth W (1989) Observation of a bacteriochlorophyll anion radical during the primary charge separation in a reaction center. Chem Phys Lett 160: 1–7

Holzapfel W, Finkele U, Kaiser W, Oesterhelt D, Scheer H, Stilz HU and Zinth W (1990) Initial electron transfer in the reaction center from *Rhodobacter sphaeroides*. Proc Natl Acad Sci USA 87: 5168–5172

Huber H, Meyer M, Nägele T, Hartl I, Scheer H, Zinth W and Wachtveitl J (1995) Primary photosynthesis in reaction centers containing 4 different types of electron accepters at site H_A. Chem Phys 197: 297–305

Huber H, Meyer M, Scheer H, Zinth W and Wachtveitl J (1998) Temperature dependence of the primary electron transfer reaction in pigment-modified bacterial reaction centers. Photosynth Res 55: 153–162

Huppmann P, Arlt T, Penzkofer H, Schmidt S, Bibikova M, Dohse B, Oesterhelt D, Wachtveitl J and Zinth W (2002) Kinetics, energetics, and electronic coupling of the primary electron transfer reactions in mutated reaction centers of *Blastochloris viridis*. Biophys J 82: 3186–3197

Huppmann P, Spörlein S, Bibikova M, Oesterhelt D, Wachtveitl J and Zinth W (2003) Electron transfer in reaction centers of *Blastochloris viridis*: Photosynthetic reactions approximating the adiabatic regime. J Phys Chem A 107: 8302–8309

Jackson JA, Lin S, Taguchi AKW, Williams JC, Allen JP and Woodbury NW (1997) Energy transfer in *Rhodobacter sphaeroides* reaction centers with the initial electron donor oxidized or missing. J Phys Chem B 101: 5747–5754

Jia YW, DiMagno TJ, Chan CK, Wang ZY, Du M, Hanson DK, Schiffer M, Norris JR, Fleming GR and Popov MS (1993) Primary charge separation in mutant reaction centers of *Rhodobacter capsulatus*. J Phys Chem 97: 13180–13191

Joo TH, Jia YW, Yu JY, Jonas DM and Fleming GR (1996) Dynamics in isolated bacterial light harvesting antenna LH2 of *Rhodobacter sphaeroides* at room temperature. J Phys Chem 100: 2399–2409

Jordan P, Fromme P, Witt HT, Klukas O, Saenger W and Krauss N (2001) Three-dimensional structure of cyanobacterial Photosystem I at 2.5 Ångstrom resolution. Nature 411: 909–917

Kirmaier C, Holten D and Parson WW (1985) Temperature and detection-wavelength dependence of the picosecond electron transfer kinetics measured in *Rhodopseudomonas sphaeroides* reaction centers resolution of new spectral and kinetic components in the primary charge-separation process. Biochim Biophys Acta 810: 33–48

Knapp EW, Fischer SF, Zinth W, Sander M, Kaiser W, Deisenhofer J and Michel H (1985) Analysis of optical-spectra from single-crystals of *Rhodopseudomonas viridis* reaction centers. Proc Natl Acad Sci USA 82: 8463–8467

Kolbasov D and Scherz A (2000) Asymmetric electron transfer in reaction centers of purple bacteria strongly depends on different electron matrix elements in the active-and inactive branches. J Phys Chem B 104: 1802–1809

Kuglstatter A, Hellwig P, Fritzsch G, Wachtveitl J, Oesterhelt D, Mäntele W and Michel H (1999) Identification of a hydrogen bond in the phe M197 -> tyr mutant reaction center of the photosynthetic purple bacterium *Rhodobacter sphaeroides* by X-ray crystallography and FTIR spectroscopy. FEBS Lett 463: 169–174

Kumble R, Palese S, Visschers RW, Dutton PL and Hochstrasser RM (1996) Ultrafast dynamics within the B820 subunit from the core LH-1 antenna complex of *Rs. rubrum*. Chem Phys Lett 261: 396–404

Lathrop EJP and Friesner RA (1994) Simulation of optical-spectra from the reaction-center of *Rhodobacter sphaeroides* — effects of an internal charge-separated state of the special pair. J Phys Chem 98: 3056–3066

Lauterwasser C, Finkele U, Scheer H and Zinth W (1991) Temperature-dependence of the primary electron-transfer in photosynthetic reaction centers from *Rhodobacter sphaeroides*. Chem Phys Lett 183: 471–477

Lin S, Jackson J, Taguchi AKW and Woodbury NW (1998) Excitation wavelength dependent spectral evolution in *Rhodobacter sphaeroides* R-26 reaction centers at low temperatures: The Q_Y transition region. J Phys Chem B 102: 4016–4022

Lin X, Murchison HA, Nagarajan V, Parson WW, Allen JP and Williams JC (1994) Specific alteration of the oxidation potential of the electron donor in reaction centers from *Rhodobacter sphaeroides*. Proc Natl Acad Sci USA 91: 10265–10269

Marcus RA (1987) Superexchange versus an intermediate bchl-mechanism in reaction centers of photosynthetic bacteria. Chem Phys Lett 133: 471–477

Marcus RA and Sutin N (1985) Electron transfers in chemistry and biology. Biochim Biophys Acta 811: 265–322

Martin JL, Breton J, Hoff AJ, Migus A and Antonetti A (1986) Femtosecond spectroscopy of electron transfer in the reaction center of the photosynthetic bacterium *Rhodopseudomonas sphaeroides* R-26 direct electron transfer from the dimeric bacteriochlorophyll primary donor to the bacteriopheophytin acceptor with a time constant of 2.8 plus or minus 0.2 picoseconds. Proc Natl Acad Sci USA 83: 957–961

McMahon BH, Muller JD, Wraight CA and Nienhaus GU (1998) Electron transfer and protein dynamics in the photosynthetic reaction center. Biophys J 74: 2567–2587

Meyer M and Scheer H (1995) Reaction centers of *Rhodobacter sphaeroides* R-26 containing C-3 acetyl and vinyl (bacterio)pheophytins at sites H_A, H_B. Photosynth Res 44: 55–65

Michel-Beyerle ME, Plato M, Deisenhofer J, Michel H, Bixon M and Jortner J (1988) Unidirectionality of charge separation in reaction centers of photosynthetic bacteria. Biochim Biophys Acta 932: 52–70

Mokhtari A, Chebira A and Chesnoy J (1990) Subpicosecond fluorescence dynamics of dye molecules. J Opt Soc Am B 7: 1551–1557

Monshouwer R, Abrahamsson M, vanMourik F and van Grondelle R (1997) Superradiance and exciton delocalization in bacterial photosynthetic light-harvesting systems. J Phys Chem B 101: 7241–7248

Moser CC, Keske JM, Warncke K, Farid RS and Dutton PL (1992) Nature of biological electron-transfer. Nature 355: 796–802

Moser CC, Keske JM, Warncke K, Farid RS and Dutton PL (1993) Electron-transfer mechanisms in reaction centers: Engineering guidelines. In: Deisenhofer J and Norris JR (eds) The Photosynthetic Reaction Center, pp 1–22. Academic Press, San Diego

Murchison HA, Alden RG, Allen JP, Peloquin JM, Taguchi AK, Woodbury NW and Williams JC (1993) Mutations designed to modify the environment of the primary electron donor of

the reaction center from *Rhodobacter sphaeroides*: Phenylalanine to leucine at l167 and histidine to phenylalanine at l168. Biochemistry 32: 3498–3505

Ogrodnik A, Keupp W, Volk M, Aumeier G and Michel-Beyerle ME (1994) Inhomogeneity of radical pair energies in photosynthetic reaction centers revealed by differences in recombination dynamics of $P^{+}H_{A}^{-}$ when detected in delayed emission and in absorption. J Phys Chem 98: 3432–3439

Parson WW and Warshel A (1993) Simulations of electron transfer in bacterial reaction centers. In: Deisenhofer J and Norris JR (eds) The Photosynthetic Reaction Center, pp 23–48. Academic Press, San Diego

Prokhorenko VI and Holzwarth AR (2000) Primary processes and structure of the Photosystem II reaction center: A photon echo study. J Phys Chem B 104: 11563–11578

Rautter J, Lendzian F, Lubitz W, Wang S and Allen JP (1994) Comparative-study of reaction centers from photosynthetic purple bacteria — electron-paramagnetic-resonance and electron-nuclear double-resonance spectroscopy. Biochemistry 33: 12077–12084

Remy A and Gerwert K (2003) Coupling of light-induced electron transfer to proton uptake in photosynthesis. Nat Struct Biol 10: 637–644

Rosker MJ, Wise FW and Tang CL (1986) Femtosecond relaxation dynamics of large molecules. Phys Rev Lett 57: 321–324

Savikhin S, Xu W, Chitnis PR and Struve WS (2000) Ultrafast primary processes in PS I from *Synechocystis* sp. PCC 6803: Roles of p700 and a(o). Biophys J 79: 1573–1586

Schenkl S, Spörlein S, Müh F, Witt H, Lubitz W, Zinth W and Wachtveitl J (2002) Selective perturbation of the second electron transfer step in mutant bacterial reaction centers. Biochim Biophys Acta 1554: 36–47

Schmidt S, Arlt T, Hamm P, Huber H, Nägele T, Wachtveitl J, Meyer M, Scheer H and Zinth W (1994) Energetics of the primary electron-transfer reaction revealed by ultrafast spectroscopy on modified bacterial reaction centers. Chem Phys Lett 223: 116–120

Schmidt S, Arlt T, Hamm P, Huber H, Nägele T, Wachtveitl J, Zinth W, Meyer M and Scheer H (1995) Primary electron-transfer dynamics in modified bacterial reaction centers containing pheophytin-a instead of bacteriopheophytin-*a*. Spectrochim Acta A 51: 1565–1578

Shkuropatov AY and Shuvalov VA (1993) Electron-transfer in pheophytin *a*-modified reaction centers from *Rhodobacter sphaeroides* (R-26). FEBS Lett 322: 168–172

Shuvalov VA and Yakovlev AG (2003) Coupling of nuclear wavepacket motion and charge separation in bacterial reaction centers. FEBS Lett 540: 26–34

Spörlein S, Zinth W and Wachtveitl J (1998) Vibrational coherence in photosynthetic reaction centers observed in the bacteriochlorophyll anion band. J Phys Chem B 102: 7492–7496

Spörlein S, Zinth W, Meyer M, Scheer H and Wachtveitl J (2000) Primary electron transfer in modified bacterial reaction centers: Optimization of the first events in photosynthesis. Chem Phys Lett 322: 454–464

Stanley RJ and Boxer SG (1995) Oscillations in the spontaneous fluorescence from photosynthetic reaction centers. J Phys Chem 99: 859–863

Stanley RJ, King B and Boxer SG (1996) Excited state energy transfer pathways in photosynthetic reaction centers .1. Structural symmetry effects. J Phys Chem 100: 12052–12059

Stowell MHB, McPhillips TM, Rees DC, Soltis SM, Abresch E and Feher G (1997) Light-induced structural changes in photosynthetic reaction center: Implications for mechanism of electron-proton transfer. Science 276: 812–816

Streltsov AM, Aartsma TJ, Hoff AJ and Shuvalov VA (1997) Oscillations within the B_L absorption-band of *Rhodobacter sphaeroides* reaction centers upon 30 femtosecond excitation at 865 nm. Chem Phys Lett 266: 347–352

Struck A and Scheer H (1990) Modified reaction centers from *Rhodobacter sphaeroides* R26 — exchange of monomeric bacteriochlorophyll with 13(2)-hydroxy- bacteriochlorophyll. FEBS Lett 261: 385–388

Struck A, Cmiel E, Katheder I and Scheer H (1990) Modified reaction centers from *Rhodobacter sphaeroides* R26 .2. Bacteriochlorophylls with modified c-3 substituents at sites B_A and B_B. FEBS Lett 268: 180–184

Trissl HW, Breton J, Deprez J, Dobek A and Leibl W (1990) Trapping kinetics, annihilation, and quantum yield in the photosynthetic purple bacterium *Rps. viridis* as revealed by electric measurement of the primary charge separation. Biochim Biophys Acta 1015: 322–333

van Brederode ME, Jones MR and van Grondelle R (1997a) Fluorescence excitation spectra of membrane-bound photosynthetic reaction centers of *Rhodobacter sphaeroides* in which the tyrosine M210 residue is replaced by tryptophan: Evidence for a new pathway of charge separation. Chem Phys Lett 268: 143–149

van Brederode ME, Jones MR, van Mourik F, van Stokkum IHM and van Grondelle R (1997b) A new pathway for transmembrane electron transfer in photosynthetic reaction centers of *Rhodobacter sphaeroides* not involving the excited special pair. Biochemistry 36: 6855–6861

van Grondelle R, Dekker JP, Gillbro T and Sundström V (1994) Energy-transfer and trapping in photosynthesis. Biochim Biophys Acta 1187: 1–65

Vasil'ev S, Orth P, Zouni A, Owens TG and Bruce D (2001) Excited-state dynamics in Photosystem II: Insights from the X-ray crystal structure. Proc Natl Acad Sci USA 98: 8602–8607

Vos MH and Martin JL (1999) Femtosecond processes in proteins. Biochim Biophys Acta 1411: 1–20

Vos MH, Lambry JC, Robles SJ, Youvan DC, Breton J and Martin JL (1991) Direct observation of vibrational coherence in bacterial reaction centers using femtosecond absorption spectroscopy. Proc Natl Acad Sci USA 88: 8885–8889

Vos MH, Rappaport F, Lambry JC, Breton J and Martin JL (1993) Visualization of coherent nuclear motion in a membrane protein by femtosecond spectroscopy. Nature 363: 320–325

Vos MH, Jones MR, Hunter CN, Breton J, Lambry JC and Martin JL (1994) Coherent dynamics during the primary electron-transfer reaction in membrane-bound reaction centers of *Rhodobacter sphaeroides*. Biochemistry 33: 6750–6757

Vos MH, Breton J and Martin JL (1997) Electronic energy transfer within the hexamer cofactor system of bacterial reaction centers. J Phys Chem B 101: 9820–9832

Wachtveitl J, Farchaus JW, Das R, Lutz M, Robert B and Mattioli TA (1993) Structure, spectroscopic, and redox properties of *Rhodobacter sphaeroides* reaction centers bearing point mutations near the primary electron donor. Biochemistry 32: 12875–12886

Wachtveitl J, Huber H, Feick R, Rautter J, Müh F and Lubitz W (1998) Electron transfer in bacterial reaction centers with an en-

ergetically raised primary acceptor: Ultrafast spectroscopy and ENDOR/TRIPLE studies. Spectrochim Acta 54: 153–162

Wang Q, Schoenlein RW, Peteanu LA, Mathies RA and Shank CV (1994) Vibrationally coherent photochemistry in the femtosecond primary event of vision. Science 266: 422–424

Warshel A (1980) Role of the chlorophyll dimer in bacterial photosynthesis. Proc Natl Acad Sci USA 77: 3105–3109

Williams JC, Alden RG, Murchison HA, Peloquin JM, Woodbury NW and Allen JP (1992) Effects of mutations near the bacteriochlorophylls in reaction centers from *Rhodobacter sphaeroides*. Biochemistry 31: 11029–11037

Woodbury NW, Becker M, Middendorf D and Parson WW (1985) Picosecond kinetics of the initial photochemical electron-transfer reaction in bacterial photosynthetic reaction centers. Biochemistry 24: 7516–7521

Woodbury NW, Peloquin JM, Alden RG, Lin X, Lin S, Taguchi AK, Williams JC and Allen JP (1994) Relationship between thermodynamics and mechanism during photoinduced charge separation in reaction centers from *Rhodobacter sphaeroides*. Biochemistry 33: 8101–8112

Xu D and Schulten K (1994) Coupling of protein motion to electron-transfer in a photosynthetic reaction-center — investigating the low-temperature behavior in the framework of the spin-boson model. Chem Phys 182: 91–117

Zhang LY and Friesner RA (1998) *Ab initio* calculation of electronic coupling in the photosynthetic reaction center. Proc Natl Acad Sci USA 95: 13603–13605

Zinth W, Kaiser W and Michel H (1983) Efficient photochemical activity and strong dichroism of single-crystals of reaction centers from *Rhodopseudomonas viridis*. Biochim Biophys Acta 723: 128–131

Zinth W, Huppmann P, Arlt T and Wachtveitl J (1998) Ultrafast spectroscopy of the electron transfer in photosynthetic reaction centres: Towards a better understanding of electron transfer in biological systems. Philos Trans Roy Soc Lond A 356: 465–476

Zouni A, Witt HT, Kern J, Fromme P, Krauss N, Saenger W and Orth P (2001) Crystal structure of Photosystem II from *Synechococcus elongatus* at 3.8 Ångstrom resolution. Nature 409: 739–743